Journal of Robotics and Control (JRC)
Volume 5, Issue 6, 2024
ISSN: 2715-5072, DOI: 10.18196/jrc.v5i6.22071

A Low-Cost High Performance Electric Vehicle Design Based on Variable Structure Fuzzy PID Control

Mohamed A. Shamseldin [1*], Medhat Araby [2], S. El-khatib [3]
[1, 3] Department of Mechanical Engineering, Future University in Egypt, Cairo, Egypt
[2] Service Manager at ARABIAT for Trading and Distribution Company
Email: [1] Mohamed.abelbbar@fue.edu.eg, [2] medhat.araby@arabiat-eg.com, [3] samah.elmetwally@fue.edu.eg
*Corresponding Author

***Abstract*—This paper introduces the design steps and implementation of Electric Vehicle (EV) based on variable structure fuzzy PID control. The role of fuzzy logic is making change in the membership function to tune the fuzzy action according to the error and change of error. The control implementation was executed using a low-cost Arduino mega 2560 and had been programed by MATLAB SIMULINK. Also, a nonlinear model for the EV was built and validated by the actual performance of the EV experimental setup. The overall EV closed loop implemented on the MATLAB SIMULINK to select the proper control parameters. The proposed variable structure fuzzy PID control had been compared to the traditional PID control to ensure robustness and reliability. The results show that the proposed control technique can deal with the EV disturbances and continuous change in the operating points.**

Keywords—Electric Vehicle; Fuzzy Logic; PID; Variable Structure.

I. INTRODUCTION

The use of electric vehicle (EV) technology is required due to the escalating environmental issues and the increasing demand for fossil fuel resources [1]-[4]. In recent years, EVs have become more and more popular due to their high efficiency, low maintenance requirements, and simple operations [5]-[9]. Urban cities now have improved sustainability and a significant reduction in pollution because of the growing EV trend. The performance of an EV has been significantly influenced by its propulsion system. Industrial and academic researchers have mainly concentrated on creating controls for the electric vehicle's drivetrain [10]-[14]. The two most important aspects, efficient performance, and desirable energy management call for thorough and targeted research. The controller should deliver the fastest possible speed while consuming the least amount of energy [15]-[18]. The fluctuating road conditions, motor characteristics, and outside disturbances make the EV system highly nonlinear, time-dependent, and uncertain. As a result, it is difficult to build a controller that completely removes external disturbances and manages uncertainty with little control signal [19]-[30].

Due to their simplicity and ease of tuning, conventional PID controllers are frequently used in a variety of industrial applications [30]-[40]. However, they do not guarantee desired dynamic performance and do not operate effectively under a variety of operating conditions. With self-tuning capabilities [40]-[45]. Due to the windup, it produces a strong control signal, which causes it to overshoot and increase as the accumulated error is unwound (compensated by errors in the other direction), and the differentiator causes noise amplification [46]-[50]. Until now, there is no definite method the select the proper parameters. So, several optimization techniques can be used to solve this problem such as Genetic Algorithm (GA), Particle Swarm Optimization (PSO), Backtracking Search Algorithm (BSA), Bee Colony Optimization (BCA), Harmony Search (HS), Ant Colony, differential evolution (DE) and COVID-19 optimization [50]-[60]

Artificial intelligence (AI) based controllers have gained importance due to their satisfactory performance in various motor control applications, including speed assessment and torque ripple minimization [61]-[64]. However, AI-based controllers suffer from drawbacks, such as large data requirements, extended learning, and training duration.

Fuzzy logic finds successful applications in a wide range of control systems, from air-conditioners and traffic lights to washing machines and large economic systems. Unlike traditional control systems that rely on precise models and objective functions, fuzzy logic control (FLC) allows for the utilization of human expertise and experience in designing controllers. The core of fuzzy control lies in the formulation of IF-THEN rules, which capture the knowledge and decision-making process of human operators.

When designing a fuzzy logic control system, several key assumptions need to be made. Firstly, it is assumed that the plant under control is observable and controllable, meaning that the necessary input, output, and state variables are available for monitoring and adjustment. Additionally, the existence of a knowledge body is assumed, which comprises linguistic rules and input-output data sets that serve as the foundation for rule extraction. Fuzzy logic control also operates under the assumption that a solution exists, although it may not necessarily be optimal. The control engineering process aims for a "good enough" solution within an acceptable range of precision, while stability and optimality are addressed implicitly rather than explicitly.

The fixed membership fuzzy cannot deal with the violent disturbances of the EV system. So, this study merges the simplicity of the traditional PID control and the fuzzy system with variable membership structure to achieve high EV performance. The proposed technique had been compared to the conventional PID control. The results provide that the proposed control can absorb the system uncertainty to track accurately the preselected trajectory.

The rest of the article organized as follows the first section demonstrates the EV design steps and the EV main components. The second section shows in detail the proposed technique. The third section displays the EV performance using the proposed control technique. The last section illustrates the paper conclusion.

II. ELECTRIC VEHICLE SYSTEM

The EV's three subsystems are primarily divided into three categories: propulsion, energy supply, and auxiliary subsystems. The vehicle controller, power electronic converter, electric motor, mechanical gearbox, sensors, and driving wheels make up the propulsion subsystem, as shown in Fig. 1. The energy supply subsystem consists of the energy source, the energy management unit, the charger unit, and other components. The auxiliary subsystem is composed of the power steering unit, the air conditioning motor and its controller, and the auxiliary supply unit. By merging the subsystems, the Electric Vehicle Drivetrain System is created. The main EV components are demonstrated in Fig. 1.

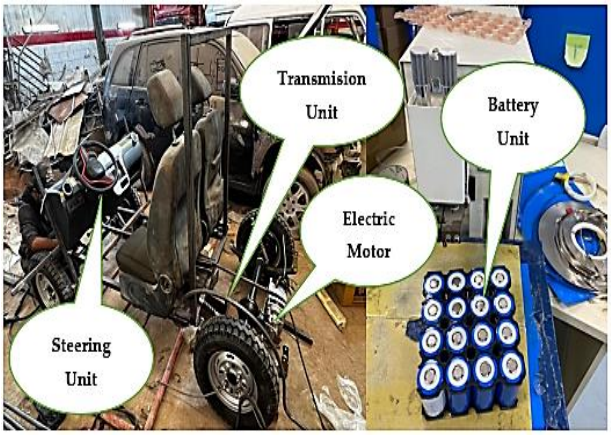

Fig. 1. A simple structure of an electric vehicle

A. Chassis Design

The cockpit design must consider the 95th percentile of a male human body to meet the ergonomic requirements for the driver. The interior dimensions of the cockpit must also be designed to maximize safety and comfort for the driver. These dimensions include the stiffness, space, and vision requirements of the cockpit, including head clearance, steering wheel position and angle, pedal locations, seat location and angles, seat belt angles, control switches and display locations.

The space frame kind of chassis design was selected as shown in Fig. 2. Because it could be prototyped at a lower cost. The chassis has undergone multiple trials of varying materials, member cross-sections, and segmentation after adhering to the aforementioned considerations. Frontal impact, side impact, rollover, and torsional stiffness stress analysis experiments were utilised in the design and modelling phases to verify the safety of the chassis. Until acceptable safety factors and deflections were obtained in every instance, the procedure was repeated.

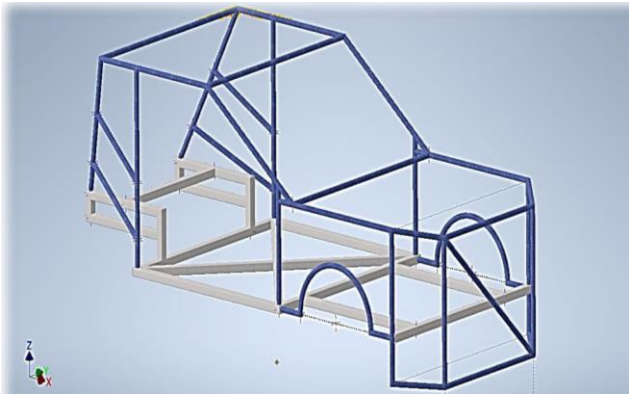

Fig. 2. A simple structure of an EV chassis

Stresses can be measured and calculated using various techniques. The common methods used are to physically apply loads to the chassis and measure the deflections by sight or by attaching strain gauges. When the deflection is known the stress can be calculated. Stresses can also be calculated using simple formulas and hand calculations, but this usually requires many simplifications to be made as demonstrated in Fig. 3.

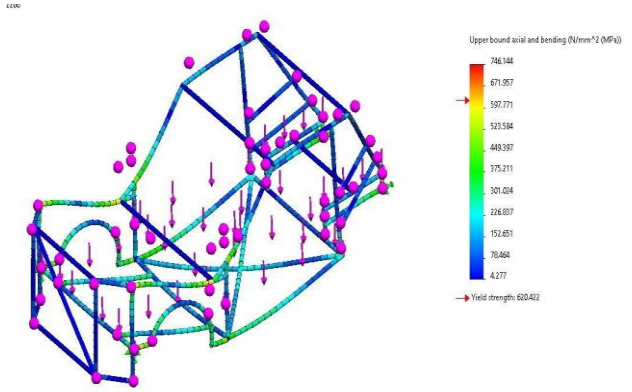

Fig. 3. A simple structure of an EV chassis

When complex structures such as chassis are analyzed, the formulas become very large and complex, therefore computer programs are required to calculate the stresses involved. When analyzing the formula SAE chassis both physical and numerical tests will be performed to calculate realistic stresses that might be experienced in the chassis under race conditions. Using both methods, comparisons can be made to verify the accuracy of the results.

Because of the complexity of the spaceframe chassis, hand numerical calculations would prove extremely lengthy. Therefore, the numerical tests will be completed using finite element analysis (FEA) software. This software allows complex numerical calculations to be performed in feasible time. Property settings required to conduct FEA can often be complicated to simulate the real conditions.

B. Suspension System

The main suspension system requirement is to isolate the passenger response from the road disturbance to achieve human ride comfort, passenger safety, and vehicle traction/braking performance. To achieve this, the ride comfort zone must be considered first. This constitutes the suspension natural frequencies to the values suggested by the ISO 2631- 1978 (E) standard (Ding et al., 2020; Suspension Geometry and Computation, n.d.), based on the expected sprung mass of the vehicle. The suspension type chosen for the present platform was the double wishbone for the front suspension and trailing arm for the rear suspension, as shown in Fig. 4. The front double wishbone was chosen for the front suspension due to its simplicity and low cost while maintaining a satisfactory ride performance for such an urban style vehicle. The rear trailing arm was chosen due to its suitability for the proposed rear individual drive arrangement. The roll centers/axis analysis and the anti-squat analysis were carried out to maintain the ride characteristics of the vehicle as shown in Fig. 5.

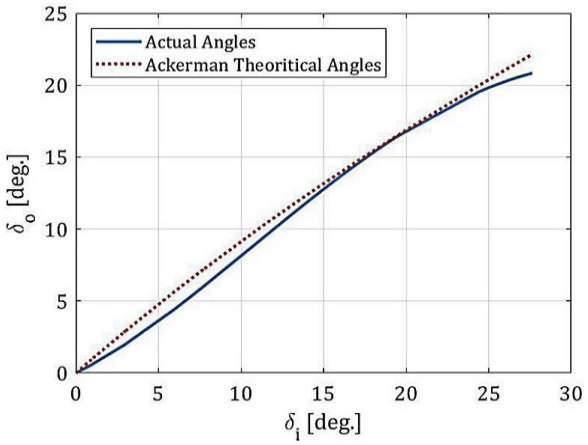

Fig. 4. Ackerman steering geometry for rack-and-pinion system

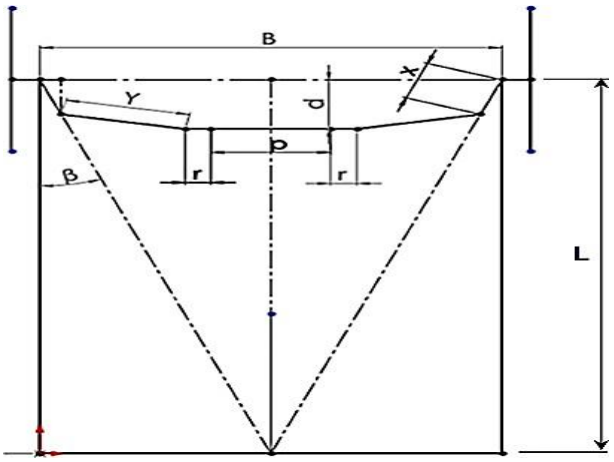

Fig. 5. The obtained relation between inner (δi) and outer (δo) steering angles compared to the Ackerman angles after optimizing the steering linkages' lengths

The quarter-car and the half-car models were used to predict the ride performance of the vehicle as demonstrated in Fig. 6. This includes the natural frequencies and locations of the bounce and pitch oscillation centers of the vehicle. This led to choosing the proper proportionality between the front and rear suspension stiffness. The final step in the suspension design procedure was checking the stresses and safety factors of the individual components of the suspension system.

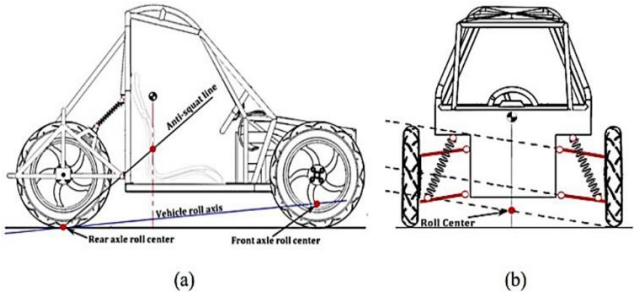

Fig. 6. System arrangement; (a) Roll axis and anti-squat analyses for rear trailing-arm suspension, (b) Roll center analysis for front double-wishbone suspension

C. Steering System

The main requirement of the steering system is to safely achieve a minimum turning radius of 4 m. Since the simplest design is the rack-and-pinion steering system, it was considered in the present work. The steering system linkages' lengths were optimized to closely achieve the Ackerman angles. This optimization considered the trigonometric equations relating the vehicle's main dimensions and the steering linkages' lengths as illustrated in Fig. 7. Stress analysis of steering components was carried out.

Fig. 7. The proposed steering system after implementation

D. Braking System

To achieve the simultaneous all-wheel lock and the minimum stopping distance requirements of the brake system, the brake proportioning should be addressed during the brake system design. Starting from the static front/rear load distribution and passing through the maximum deceleration level, the front-to-rear brake force ratio, namely brake proportioning, is constituted. The hydraulic brake design parameters should be selected to achieve the desired brake proportioning as well as the required total brake force. Along with all brake design parameters, the selection of front/rear discs' effective radii and the front/rear wheels pistons' diameters gives the easiest way to achieve those two conditions. Fig. 8 shows the brake proportioning line for the present vehicle.

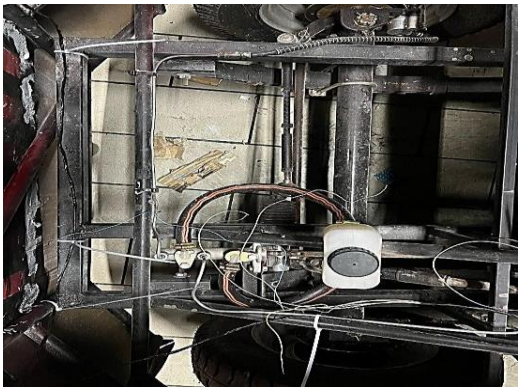

Fig. 8. Full braking system

III. FINAL EV ASSEMBLY AND MATHEMATICAL MODEL

The nonlinear state space model of proposed EV can be considered as follows.

$$\dot{X} = f(X) + g(X)u \tag{1}$$

$$X = \begin{bmatrix} x1 \\ x2 \end{bmatrix} = \begin{bmatrix} i \\ w \end{bmatrix} \tag{2}$$

$$f(x) = \begin{bmatrix} \frac{-(R_a+R_f)}{L_a+L_f}x_1 - \frac{L_{af}}{L_a+L_f}x_1.x_2 \\ \frac{1}{J+m(\frac{r^2}{G^2})}\left[L_{af}x_1^2 - Bx_2 - \frac{r}{G}(\mu_{rr}mg + \frac{1}{2}\rho AC_d\left(\frac{r^2}{G^2}\right){x_2}^2 + mgsin(\varphi))\right] \end{bmatrix} \tag{3}$$

$$g(x) = \begin{bmatrix} \frac{1}{L_a+L_f} \\ 0 \end{bmatrix} \tag{4}$$

$$v = \omega \times \frac{r}{G} \tag{5}$$

where m is the mass of the electric vehicle, g is the gravity acceleration, v the driving velocity of the vehicle, μ_{rr} the rolling resistance coefficient, ρ the air density, A the frontal area of the vehicle, C_d the drag coefficient and φ the hillclimbing angle, i is considered the armature and field current, ω the angular speed of the motor, La the armature inductance, R_a the armature resistance, L_f the field winding inductance, R_f the field winding resistance, Laf the mutual inductance among the field and armature windings, B the viscous coefficient, J the moment of inertia of the motor, T_L the external torque and V the input voltage. Table I describes the EV parameters and specifications.

TABLE I. PARAMETERS OF THE NONLINEAR EV SYSTEM

Symbol	Value	Symbol	value
L_a+L_f	6.008 mH	m	400 kg
R_a+R_f	0.12 Ω	A	1.8 m2
L_{af}	0.001 mH	ρ	1.25 (kg/m3)
i	25	φ	0°
V	0:48 V	C_d	0.3
B	0.0002 N.M.s	μ_{rr}	0.015
J	0.05 Kg.m2	G	5
ω	50 Km/h	r	0.35 m

The EV system is classified into two main sub-systems. The first is the electric motor drive system and the second is the chassis of the body with suspension parts (Fig. 9 and Fig. 10). The nonlinearity source comes from the mutual inductance of the motor winding, mechanical transmission, measurement uncertainty. The purpose of the proposed controllers absorbs external disturbances such as aerodynamic resistance, road variations, and several operating points of speed. Moreover, overcoming internal disturbances such as the mentioned nonlinearity resources.

Fig. 9. EV SolidWorks design

Fig. 10. The final EV after overall manufacturing

A comparison between the response of the proposed model state space and the EV experimental setup response. The result of this comparison is demonstrated in Fig. 11. It can be noted that the proposed model simulates significantly the EV experimental setup but the response of EV experimental setup suffers from high noise due to the system uncertainty.

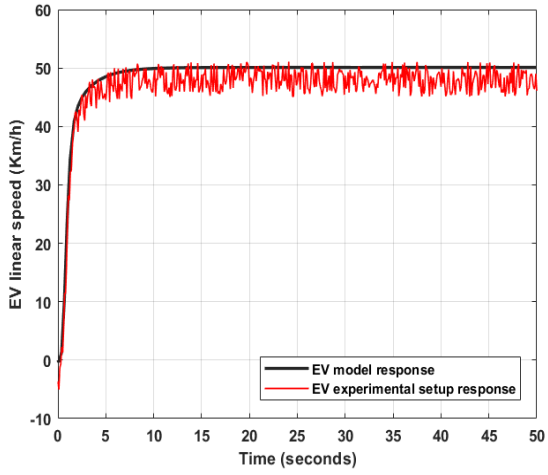

Fig. 11. The EV linear speed response for the proposed model and the EV experimental setup

IV. VARIABLE STRUCTURE FUZZY PID CONTROL

Two different categories of adaptive fuzzy controllers exist. The first kind adjusts the fuzzy system's rules, which is why it is sometimes referred to as a self-organizing controller

or variable structure controller. The second class of fuzzy controllers, known as self-tuning controllers, allows for online scaling factor modification. The earlier experiments demonstrated that the first type of adaptive fuzzy controller is superior than the second type in terms of effectiveness. However, compared to the second type of adaptive fuzzy controller, the first type requires the designer to develop the fuzzy system from scratch without the use of a software toolbox.

The proposed technique has an adaptive mechanism to tune the centroid of rule base membership online based on the optimal model reference adaptive system.

Fig. 12 illustrates the general structure of variable structure fuzzy PID control.

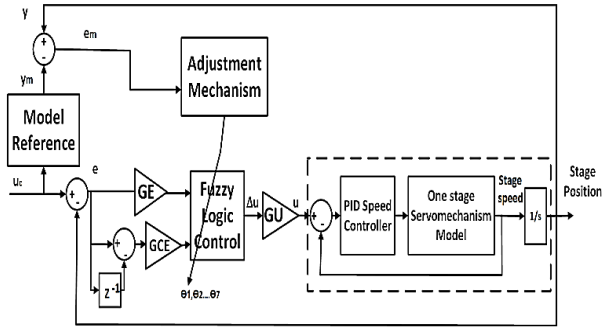

Fig. 12. Variable Structure Fuzzy PID (VSFPID) control

The variable structure fuzzy PD control input/output relationship can be described as follows.

$$u(s) = GU.\Delta u(s) \tag{6}$$

$$\Delta u(s) = \underline{\boldsymbol{\theta}}^{\boldsymbol{T}}\underline{\mathfrak{z}}(\underline{\boldsymbol{x}}) \tag{7}$$

$$E(s) = GE.e(s) \tag{8}$$

$$CE(s) = GCE.ce(s) \tag{9}$$

$$GE = 1,\ GCE = \frac{k_d}{k_p},\ GU = k_p \tag{10}$$

where u(s) is the output fuzzy controller, Where $\underline{\boldsymbol{\theta}}^{\boldsymbol{T}}$is the centroid vector of the output membership function, $\underline{\mathfrak{z}}(\underline{\boldsymbol{x}})$ is the vector of the fuzzy basis function, $x \in [-1, 1]$, and GU is the scaling factor for fuzzy PD controller. Inputs of the fuzzy controller are scaled using, GCE scaling factors also known as fuzzy gains, $e(s)$ is the error between the reference position and the actual position of stage and $ce(s)$ is the change of this error (Fig. 13). Here, we introduce a reference model in the structure of the fuzzy controller to generate model error given by

$$e_m(s) = y(s) - y_m(s) \tag{11}$$

In equation (7), the $y(s)$ is the actual system output, the $y_m(s)$ stands for the desired performance and $e_m(s)$ considers the difference between the actual process value and the expected value of output. The reference model can be a first or second-order system. The model reference transfer function contains the desired response of the system such as the desired damping ratio, the desired natural frequency, the desired rise time, the desired settling time, and the desired overshoot. If the order of the reference model is a stable first-order system as the following transfer function.

$$\frac{y_m(s)}{u_c(s)} = \frac{k_m}{t_m s+1} \tag{12}$$

where u_c is the reference position, y_m is the output of the reference model, k_m represents the DC gain of the system ration between the input signal and the steady-state value of output and T_m is the time constant which measures how quickly a first-order system response to a unit step input.

The MIT rule is the original approach to model reference adaptive control. The name is derived from the fact that it was developed at the Instrumentation Laboratory (now the Draper Laboratory) at MIT. To adjust parameters in such a way that the loss function is minimized.

$$j(\underline{\boldsymbol{\theta}}) = \frac{1}{2}e_m^2 \tag{13}$$

To make j small, it is reasonable to change the parameters in the direction of the negative gradient of j, that is,

$$\frac{d\underline{\boldsymbol{\theta}}}{dt} = -\gamma\frac{\partial j}{\partial \underline{\boldsymbol{\theta}}} = -\gamma e_m\frac{\partial e_m}{\partial \underline{\boldsymbol{\theta}}} \tag{14}$$

Where γ stands for the adaptation gain while $\underline{\boldsymbol{\theta}}$ is the centroid vector of the output membership function.

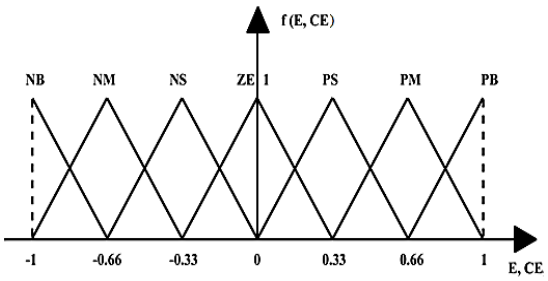

Fig. 13. The input of membership functions (error and change of error)

Fig. 14 demonstrates the adaptive output membership functions for VSFC. The linguistic labels of the outputs are {NB(θ_1), NM(θ_2), NS(θ_3), ZE(θ_4), PS(θ_5), PM(θ_6), PB(θ_7)}. The output membership's centers are not fixed and change continuously through a certain range to prevent the overlapping between the memberships.

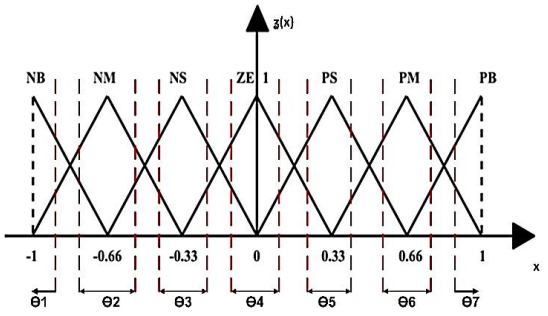

Fig. 14. The adaptive output membership functions

From the adaptive output of the membership function can outcome the following equations.

$$\underline{\theta}(0) = [\,-1\ -0.66\ -0.33\ 0\ 0.33\ 0.66\ 1\,] \tag{15}$$

$$\underline{\boldsymbol{\theta}} = [\theta_1\ \theta_2\ \theta_3\ \theta_4\ \theta_5\ \theta_6\ \theta_7] \tag{16}$$

The used defuzzification technique is the center of gravity.

$$u(nT) = \frac{\sum_{j=1}^{n} u(u_j)u_j}{\sum_{j=1}^{n} u(u_j)} = \underline{\theta}^T \underline{\zeta}(\underline{x}) \quad (17)$$

where $u\ (u_j)$ membership grad of the element u_j, $u(nT)$ is the fuzzy control output, n is the number of discrete values on the universe of discourse. Table II summarizes the adaptive rule base of VS fuzzy system.

TABLE II. ADAPTIVE MEMBERSHIP

E/CE	NB	NM	NS	ZE	PS	PM	PB
NB	NB(θ_1)	NB(θ_1)	NB(θ_1)	NB(θ_1)	NM(θ_2)	NS(θ_3)	ZE(θ_4)
NM	NB(θ_1)	NB(θ_1)	NB(θ_1)	NM(θ_2)	NS(θ_3)	ZE(θ_4)	PS(θ_5)
NS	NB(θ_1)	NB(θ_1)	NM(θ_2)	NS(θ_3)	ZE(θ_4)	PS(θ_5)	PM(θ_6)
ZE	NB(θ_1)	NM(θ_2)	NS(θ_3)	ZE(θ_4)	PS(θ_5)	PM(θ_6)	PB(θ_7)
PS	NM(θ_2)	NS(θ_3)	ZE(θ_4)	PS(θ_5)	PM(θ_6)	PB(θ_7)	PB(θ_7)
PM	NS(θ_3)	ZE(θ_4)	PS(θ_5)	PM(θ_6)	PB(θ_7)	PB(θ_7)	PB(θ_7)
PB	ZE(θ_4)	PS(θ_5)	PM(θ_6)	PB(θ_7)	PB(θ_7)	PB(θ_7)	PB(θ_7)

V. EXPERIMENTAL RESULTS

The performance of the suggested controller for the EV in the presence of both internal and external disturbances is shown in this section. To ensure that the suggested controllers were flexible and robust, a number of experiments were run. In the first test, the dynamic response of each control method is measured at a single operating point of speed.

The effectiveness of PID, or variable structure fuzzy PID (VSFPID) control in tracking the new Highway Fuel Economy Driving Schedule (HWFET) speed (km/h) test is shown in Fig. 14. It is clear that the speed profile is accurately tracked by VSFPID control. Furthermore, the PID control is unable to keep up with the speed profile's constant fluctuations. In order to verify that the VSFPID control has a short settling time and smooth behavior in comparison to alternative control techniques without an adaptive mechanism, a zoomed region was captured between 300 and 500 seconds, as shown in Fig. 15.

The incapacity of PID control to overcome system uncertainty and internal and external disturbances is the cause of its subpar performance. Furthermore, when the system experiences abrupt changes, like variable structure fuzzy logic, these controllers without adaptive mechanisms built into the auto-tuning PID controller cause the parameters to continuously adjust.

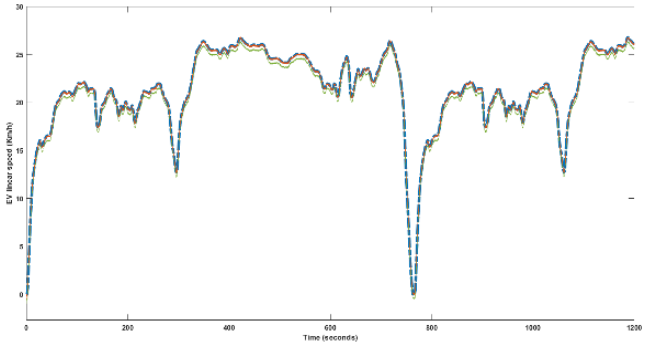

Fig. 15. The Highway Fuel Economy Driving Schedule (HWFET)

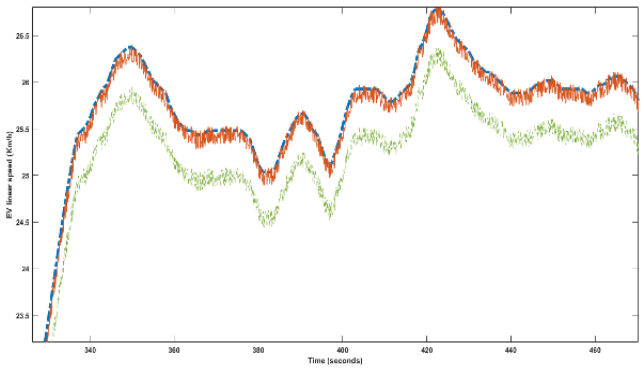

Fig. 16. Zoomed area for Fig. 15

Fig. 17 shows the Performance of the PID and VSFPID control to track The EPA Urban Dynamometer Driving Schedule (UDDS) test. It is noticed that the VSFPID controller tracks accurately its reference velocity although the violent change in the reference speed and nonlinearity resources of the EV. In the case of the PID controller cannot track the profile where the gap between the reference and the actual velocity is high.

Fig. 18 illustrates a zoomed area demonstrates the difference between the reference and the actual velocity. It can be noted that the error in case of the VSFPID control is very small compared to the PID control case.

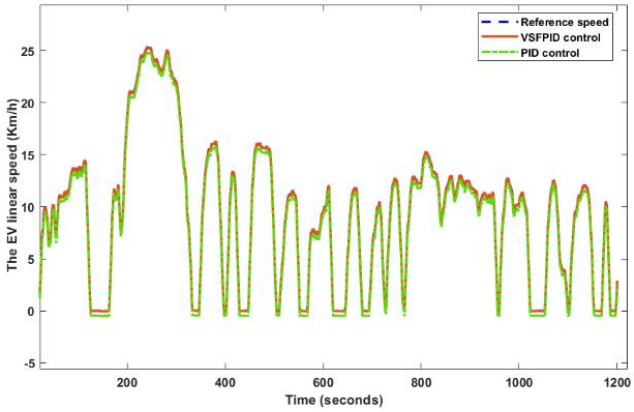

Fig. 17. The EPA Urban Dynamometer Driving Schedule (UDDS) test

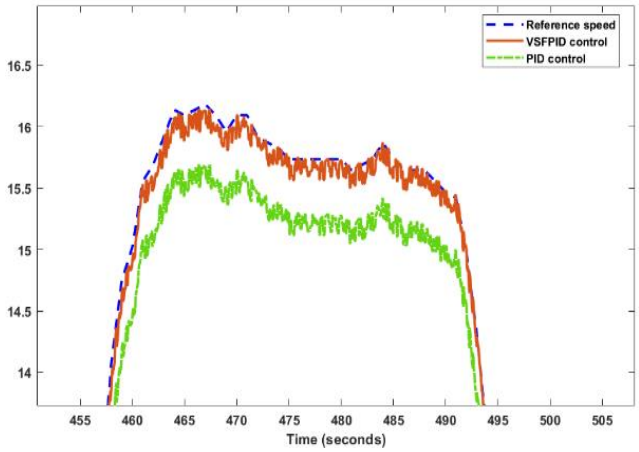

Fig. 18. Zoomed area for Fig. 17

Fig. 19 demonstrates the performance of PID, variable structure fuzzy PID (VSFPID) control to track New European Drive Cycle (NEDC) speed (Km/h) test. It is obvious that VSFPID control tracks accurately the speed profile. Also, the PID control cannot track the continuous changes in the speed profile. A zoomed area was taken from 300 seconds to 500 seconds to ensure that the VSFPID control has a small settling time and smooth behavior compared to other control technique without an adaptive mechanism as demonstrated in Fig. 20.

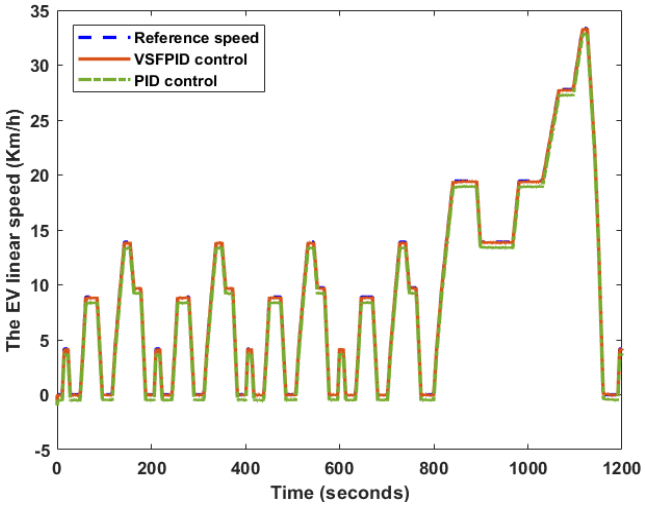

Fig. 19. New European Drive Cycle (NEDC)

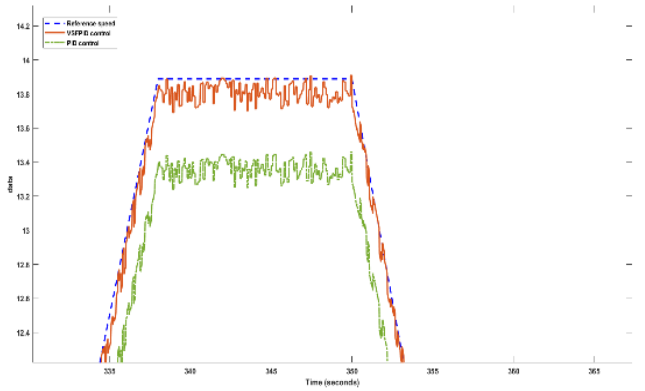

Fig. 20. Zoomed area for Fig. 20

VI. CONCLUSIONS

The design and implementation of electric vehicles (EVs) based on variable structure fuzzy PID control are presented in this work. Fuzzy logic's job is to adjust the membership function so that the fuzzy action is tuned based on error and error change. MATLAB SIMULINK was used to program an inexpensive Arduino Mega 2560, which was used to carry out the control implementation. Additionally, a nonlinear model for the EV was developed and verified by the experimental setup's real performance. To choose the appropriate control parameters, the entire EV closed loop was developed on the MATLAB SIMULINK. To verify robustness and reliability, the suggested variable structure fuzzy PID control was contrasted with the conventional PID control. The outcomes demonstrate that the suggested control strategy is capable of handling EV disruptions and ongoing changes to the operating points.

REFERENCES

[1] R. He, Y. Yan, and D. Hu, "Optimised adaptive control methodology for mode transition of hybrid electric vehicle based on the dynamic characteristics analysis," *Veh. Syst. Dyn.*, vol. 59, no. 8, pp. 1282–1303, 2021, doi: 10.1080/00423114.2020.1752923.

[2] M. H. B. Chaleshtari, E. Norouzi, and H. Ahmadi, "Optimizing control motion of a human arm with PSO-PID controller," *J. Comput. Appl. Res. Mech. Eng.*, vol. 7, no. 1, pp. 23–34, 2017, doi: 10.22061/JCARME.2017.645.

[3] Y. Gong, Y. Liu, and Z. Tang, "Path tracking of unmanned vehicle based on parameters self-tuning fuzzy control," *2013 IEEE Int. Conf. Cyber Technol. Autom. Control Intell. Syst. IEEE-CYBER 2013*, pp. 52–57, 2013, doi: 10.1109/CYBER.2013.6705419.

[4] C. Abeykoon, "Control Engineering Practice Single screw extrusion control : A comprehensive review and directions for improvements," *Control Eng. Pract.*, vol. 51, pp. 69–80, 2016, doi: 10.1016/j.conengprac.2016.03.008.

[5] T. Arora and Y. Gigras, "A Survey Of Comparison Between Various Meta -," I*nt. J. Comput. Eng. Sci.*, vol. 3, no. 2, pp. 62–66, 2013.

[6] P. P. Du, H. Su, and G. Y. Tang, "Friction compensation control for electric power steering systems," *Proc. - 2018 IEEE Int. Conf. Ind. Electron. Sustain. Energy Syst. IESES 2018*, pp. 212–217, 2018, doi: 10.1109/IESES.2018.8349876.

[7] M. A. Shamseldin, M. Salah, A. G. Mohamed, and M. A. A. Ghany, "A COVID-19 Based on Fractional Order Integral-Tilt Derivative Controller for Nonlinear Servomechanism Model," *Int. J. Electr. Eng. Comput. Sci.*, vol. 5, pp. 175–182, 2023, doi: 10.37394/232027.2023.5.19.

[8] Z.-J. Guo and X.-Y. Kang, "Modeling and Analysis of Vehicle with Wind-solar Photovoltaic Hybrid Generating System," in *4th International Conference on Sustainable Energy and Environmental Engineering*, pp. 566–570, 2016, doi: 10.2991/icseee-15.2016.95.

[9] Y. Qi, H. Dai, P. Wu, F. Gan, and Y. Ye, "RSFT-RBF-PSO: a railway wheel profile optimisation procedure and its application to a metro vehicle," *Veh. Syst. Dyn.*, vol. 60, no. 10, pp. 3398–3418, 2022, doi: 10.1080/00423114.2021.1955135.

[10] P. Rodriguez-ayerbe, D. Dumur, S. Lavernhe, P. Rodriguez-ayerbe, D. Dumur, and S. Lavernhe, "Axis control using model predictive control : identification and friction effect reduction Axis control using model predictive control : identification and friction effect reduction," in *3rd International Conference on Virtual Machining Process Technology*, 2014.

[11] R. Papdeja and P. Sankala, "Modelling and Simulation of Three Phase Brushless DC Motor With Using Model Reference Adaptive Controller," *Int. J. Invent. Comput. Sci. Eng.*, vol. 1, no. 3, 2014.

[12] M. R. Awal, M. Jusoh, M. N. Sakib, F. S. Hossain, M. R. Che Beson, and S. A. Aljunid, "Design and implementation of Vehicle Mounted Wind Turbine," *ARPN J. Eng. Appl. Sci.*, vol. 10, no. 19, pp. 8699–8706, 2015.

[13] A. . Ouda and A. Mohamed, "Autonomous Fuzzy Heading Control for a Multi-Wheeled Combat Vehicle," *Int. J. Robot. Control Syst.*, vol. 1, no. 1, pp. 90–101, Apr. 2021, doi: 10.31763/ijrcs.v1i1.286.

[14] S. A. Deraz, "Genetic Tuned PID Controller Based Speed Control of DC Motor Drive," *IJETT*, vol. 17, no. 2, pp. 88–93, 2014.

[15] M. A. Shamseldin, "Adaptive Controller with PID, FOPID, and NPID Compensators for Tracking Control of Electric – Wind Vehicle Mohamed," *J. Robot. Control*, vol. 3, no. 5, p. 546, 2022.

[16] M. A. Shamseldin, "Optimal Covid-19 Based PD/PID Cascaded Tracking Control for Robot Arm driven by BLDC Motor," *Wseas Trans. Syst.*, vol. 20, pp. 217–227, 2021, doi: 10.37394/23202.2021.20.24.

[17] M. A. Shamseldin *et al*., "A New Design Identification and Control Based on GA Optimization for an Autonomous Wheelchair," *Robotics*, vol. 11, no. 5, p. 101, 2022.

[18] M. A. Shamseldin, "Optimal Coronavirus Optimization Algorithm Based PID Controller for High Performance Brushless DC Motor," *Algorithms Artic.*, vol. 14, p. 17, 2021.

[19] Y. Zahraoui, M. Akherraz, and A. Ma'arif, "A Comparative Study of Nonlinear Control Schemes for Induction Motor Operation Improvement," *Int. J. Robot. Control Syst.*, vol. 2, no. 1, pp. 1–17, 2021, doi: 10.31763/ijrcs.v2i1.521.

[20] E. S. Rahayu, A. Ma'arif, and A. Çakan, "Particle Swarm Optimization (PSO) Tuning of PID Control on DC Motor," *Int. J. Robot. Control Syst.*, vol. 2, no. 2, pp. 435–447, 2022.

[21] F. Piltan, A. Taghizadegan, and N. B. Sulaiman, "Modeling and Control of Four Degrees of Freedom Surgical Robot Manipulator Using MATLAB/SIMULINK," *International Journal of Hybrid Information Technology*, vol. 8, no. 11, pp. 47–78, 2015.

[22] X. Wei-hong, C. Li-jia, and Z. Chun-lai, "Review of Aerial Manipulator and its Control," *Int. J. Robot. Control Syst.*, vol. 1, no. 3, pp. 308–325, 2021, doi: 10.31763/ijrcs.v1i3.363.

[23] M. Drive, "Modeling and Analysis of PI Controller Based Speed Control of Brushless DC Motor Drive," *IJESRT*, vol. 2, no. 9, pp. 7–12, 2013.

[24] A. Info, "A Survey of Control Methods for Quadrotor UAV," *Int. J. Robot. Control Syst.*, vol. 2, no. 4, pp. 652–664, 2022.

[25] C. S. R. Reddy and M. S. Kalavathi, "Performance Analysis of BLDC Motor Drive using New Simulation Model with Fuzzy and ANFIS Speed Controllers," *Glob. J. Res. Eng. F Electr. Electron. Eng*., vol. 14, no. 4, 2014.

[26] M. A. Abdel Ghany and M. A. Shamseldin, "Parallel distribution compensation PID based on Takagi-Sugeno fuzzy model applied on Egyptian load frequency control," *Int. J. Electr. Comput. Eng*., vol. 10, no. 5, pp. 5274–5287, 2020, doi: 10.11591/IJECE.V10I5.PP5274-5287.

[27] A. A. Kesarkar and N. Selvaganesan, "Systems Science & Control Engineering Tuning of optimal fractional-order PID controller using an artificial bee colony algorithm," *Syst. Sci. Control Eng*., vol. 2583, no. November, 2015, doi: 10.1080/21642583.2014.987480.

[28] L. M. El-Tehewy, M. A. Shamseldin, M. Sallam, and A. M. Abdel Ghany, "A Modified Model Reference Adaptive Control for High-Performance Pantograph Robot Mechanism," *Wseas Trans. Appl. Theor. Mech.*, vol. 16, pp. 193–203, 2021, doi: 10.37394/232011.2021.16.22.

[29] M. A. Shamseldin, M. Sallam, A. M. Bassiuny, and A. A. Ghany, "Real-time implementation of an enhanced nonlinear PID controller based on harmony search for one-stage servomechanism system," *Journal of Mechanical Engineering and Sciences*, vol. 12, no. 4, pp. 4161-4179, 2018.

[30] A. L. Elshafei, K. A. El-Metwally, and A. A. Shaltout, "A variable-structure adaptive fuzzy-logic stabilizer for single and multi-machine power systems," *Control Eng. Pract.*, vol. 13, no. 4, pp. 413–423, 2005, doi: 10.1016/j.conengprac.2004.03.017.

[31] V. Pshikhopov and M. Medvedev, "Position-path control of a vehicle," *Path Planning for Vehicles Operating in Uncertain 2D Environments*, pp. 1-23, 2017, doi: 10.1016/B978-0-12-812305-8.00001-6.

[32] R. Sharma, S. Bhasin, P. Gaur, and D. Joshi, "A switching-based collaborative fractional order fuzzy logic controllers for robotic manipulators," *Appl. Math. Model.*, vol. 73, pp. 228–246, 2019, doi: 10.1016/j.apm.2019.03.041.

[33] M. A. George, D. V. Kamat, and C. P. Kurian, "Electric vehicle speed tracking control using an ANFIS-based fractional order PID controller," *Journal of King Saud University-Engineering Sciences*, vol. 36, no. 4, pp. 256-264, 2022, doi: 10.1016/j.jksues.2022.01.001.

[34] A. X. R. Irudayaraj *et al.*, "A Matignon's theorem based stability analysis of hybrid power system for automatic load frequency control using atom search optimized FOPID controller," *IEEE Access*, vol. 8, pp. 168751–168772, 2020, doi: 10.1109/ACCESS.2020.3021212.

[35] M. U. Jan, A. Xin, M. A. Abdelbaky, H. U. Rehman, and S. Iqbal, "Adaptive and Fuzzy PI Controllers Design for Frequency Regulation of Isolated Microgrid Integrated with Electric Vehicles," *IEEE Access*, vol. 8, no. 1, pp. 87621–87632, 2020, doi: 10.1109/ACCESS.2020.2993178.

[36] I. S. Akkizidis, G. N. Roberts, P. Ridao, and J. Batlle, "Designing a Fuzzy-like PD controller for an underwater robot," *Control Eng. Pract.*, vol. 11, no. 4, pp. 471–480, 2003, doi: 10.1016/S0967-0661(02)00055-2.

[37] A. G.Preethi and A. B.Santhi, "Study on Techniques of Earthquake Prediction," *Int. J. Comput. Appl.*, vol. 29, no. 4, pp. 55–58, 2011, doi: 10.5120/3549-4867.

[38] A. Ghanbari, S. M. R. Kazemi, F. Mehmanpazir, and M. M. Nakhostin, "A cooperative ant colony optimization-genetic algorithm approach for construction of energy demand forecasting knowledge-based expert systems," *Knowledge-Based Syst.*, vol. 39, no. 2013, pp. 194–206, 2013, doi: 10.1016/j.knosys.2012.10.017.

[39] X. Xu, M. Wang, P. Xiao, J. Ding, and X. Zhang, "In-Wheel Motor Control System for Four-Wheel Drive Electric Vehicle Based on CR-GWO-PID Control," *Sensors*, vol. 23, no. 19, 2023, doi: 10.3390/s23198311.

[40] R. Zhai, P. Xiao, R. Zhang, and J. Ju, "In-wheel motor control system used by four-wheel drive electric vehicle based on whale optimization algorithm-proportional–integral–derivative control," *Adv. Mech. Eng.*, vol. 14, no. 6, pp. 1–16, 2022, doi: 10.1177/16878132221104574.

[41] T. H. S. Li and Y. C. Huang, "MIMO adaptive fuzzy terminal sliding-mode controller for robotic manipulators," *Inf. Sci. (Ny).*, vol. 180, no. 23, pp. 4641–4660, 2010, doi: 10.1016/j.ins.2010.08.009.

[42] A. Bahadir and Ö. Aydoğdu, "Modeling of a brushless dc motor driven electric vehicle and its pid-fuzzy control with dSPACE," *Sigma J. Eng. Nat. Sci.*, vol. 41, no. 1, pp. 156–177, 2023, doi: 10.14744/sigma.2023.00015.

[43] R. C. Dorf and R. H. Bishop. *Modern control systems solution manual*. Addison-Wesley, 1998.

[44] E. M. Ahmed, E. A. Mohamed, A. Elmelegi, M. Aly, and O. Elbaksawi, "Optimum Modified Fractional Order Controller for Future Electric Vehicles and Renewable Energy-Based Interconnected Power Systems," *IEEE Access*, vol. 9, pp. 29993–30010, 2021, doi: 10.1109/ACCESS.2021.3058521.

[45] J. Peng and R. Dubay, "Identification and adaptive neural network control of a DC motor system with dead-zone characteristics," *ISA Trans.*, vol. 50, no. 4, pp. 588–598, 2011, doi: 10.1016/j.isatra.2011.06.005.

[46] K. Premkumar and B. V. Manikandan, "Fuzzy PID supervised online ANFIS based speed controller for brushless dc motor," *Neurocomputing*, vol. 157, pp. 76–90, 2015, doi: 10.1016/j.neucom.2015.01.032.

[47] I. Silva and J. E. Naranjo, "A systematic methodology to evaluate prediction models for driving style classification," *Sensors*, vol. 20, no. 6, pp. 1–21, 2020, doi: 10.3390/s20061692.

[48] A. C. Sánchez, J. F. Figueroa-Rodríguez, A. G. Fuentes-Covarrubias, R. Fuentes-Covarrubias, and S. K. Gadi, "Recycling and updating an educational robot manipulator with open-hardware-architecture," *Sensors*, vol. 20, no. 6, pp. 1–22, 2020, doi: 10.3390/s20061694.

[49] J. R. García-Martínez, E. E. Cruz-Miguel, R. V. Carrillo-Serrano, F. Mendoza-Mondragón, M. Toledano-Ayala, and J. Rodríguez-Reséndiz, "A PID-type fuzzy logic controller-based approach for motion control applications," *Sensors*, vol. 20, no. 18, pp. 1–19, 2020, doi: 10.3390/s20185323.

[50] L. Xu, Z. Wang, Y. Liu, and L. Xing, "Energy allocation strategy based on fuzzy control considering optimal decision boundaries of standalone hybrid energy systems," *J. Clean. Prod.*, vol. 279, p. 123810, 2021, doi: 10.1016/j.jclepro.2020.123810.

[51] P. Swethamarai and P. Lakshmi, "Adaptive-Fuzzy Fractional Order PID Controller-Based Active Suspension for Vibration Control," *IETE J. Res.*, vol. 68, no. 5, pp. 3487–3502, 2022, doi: 10.1080/03772063.2020.1768906.

[52] M. Veysi, J. Aghaei, M. Shasadeghi, R. Razzaghi, B. Bahrani, and D. J. Ryan, "Energy-Efficient Speed Control of Electric Vehicles: Linear Matrix Inequality Approach," *IEEE Trans. Veh. Technol.*, vol. 69, no. 10, pp. 10469–10483, 2020, doi: 10.1109/TVT.2020.3008500.

[53] X. Wu, Y. Xu, J. Liu, C. Lv, J. Zhou, and Q. Zhang, "Characteristics analysis and fuzzy fractional-order PID parameter optimization for primary frequency modulation of a pumped storage unit based on a multi-objective gravitational search algorithm," *Energies*, vol. 13, no. 1, 2019, doi: 10.3390/en13010137.

[54] O. Castillo, F. Valdez, J. Soria, L. Amador-Angulo, P. Ochoa, and C. Peraza, "Comparative study in fuzzy controller optimization using bee colony, differential evolution, and harmony search algorithms," *Algorithms*, vol. 12, no. 1, 2019, doi: 10.3390/a12010009.

[55] A. Mughees and S. A. Mohsin, "Design and Control of Magnetic Levitation System by Optimizing Fractional Order PID Controller Using Ant Colony Optimization Algorithm," *IEEE Access*, vol. 8, pp. 116704–116723, 2020, doi: 10.1109/ACCESS.2020.3004025.

[56] M. Rabah, A. Rohan, Y. J. Han, and S. H. Kim, "Design of fuzzy-PID controller for quadcopter trajectory-tracking," *Int. J. Fuzzy Log. Intell.*

Syst., vol. 18, no. 3, pp. 204–213, 2018, doi: 10.5391/IJFIS.2018.18.3.204.

[57] Z. Zhang, L. Tang, W. Hao, and Q. Yuan, "Differential power steering control for in-wheel motored electric vehicle based on variable universe fuzzy PID," *J. Automot. Saf. Energy*, vol. 10, no. 2, pp. 169–177, 2019, doi: 10.3969/j.issn.1674-8484.2019.02.004.

[58] R. E. Precup *et al*., "Model-based fuzzy control results for networked control systems," *Reports Mech. Eng.*, vol. 1, no. 1, pp. 10–25, 2020, doi: 10.31181/rme200101010p.

[59] O. Domansky, R. Sotner, L. Langhammer, J. Jerabek, C. Psychalinos, and G. Tsirimokou, "Practical Design of RC Approximants of Constant Phase Elements and Their Implementation in Fractional-Order PID Regulators Using CMOS Voltage Differencing Current Conveyors," *Circuits, Syst. Signal Process.*, vol. 38, no. 4, pp. 1520–1546, 2019, doi: 10.1007/s00034-018-0944-z.

[60] X. Ding, R. Li, Y. Cheng, Q. Liu, and J. Liu, "Design of and research into a multiple-fuzzy pid suspension control system based on road recognition," *Processes*, vol. 9, no. 12, 2021, doi: 10.3390/pr9122190.

[61] S. Kapoulea, V. Bizonis, P. Bertsias, C. Psychalinos, A. Elwakil, and I. Petráš, "Reduced active components count electronically adjustable fractional-order controllers: Two design examples," *Electron.*, vol. 9, no. 1, 2020, doi: 10.3390/electronics9010063.

[62] J. Zhang, C. Li, Q. Jia, and R. Gao, "Research on the Adaptive PID Speed Control Method for Hub Motors," *Mob. Inf. Syst.*, vol. 2022, 2022, doi: 10.1155/2022/4979824.

[63] C. Sun, Z. Deng, W. Chu, S. Li, and D. Cao, "Acclimatizing the Operational Design Domain for Autonomous Driving Systems," *IEEE Intell. Transp. Syst. Mag.*, vol. 14, no. 2, pp. 10–24, 2022, doi: 10.1109/MITS.2021.3070651.

[64] S. Barakat, A. I. Osman, E. Tag-Eldin, A. A. Telba, H. M. Abdel Mageed, and M. M. Samy, "Achieving green mobility: Multi-objective optimization for sustainable electric vehicle charging," *Energy Strateg. Rev.*, vol. 53, p. 101351, 2024, doi: 10.1016/j.esr.2024.101351.